



Transport rate and bed profile computations for clay–silt–gravel mixture

Umesh K. Singh^{1,2} · Z. Ahmad¹

Received: 22 December 2018 / Accepted: 8 July 2019 / Published online: 18 July 2019
© Springer-Verlag GmbH Germany, part of Springer Nature 2019

Abstract

Identification of parameters governing sediment transport is important, as its understanding can greatly assist in resolving the issues caused by sediment transport in the riverine system. This paper presents the results of an experimental study for the computation of bed load transport rate and suspended load transport rate along with transient bed profile for a cohesive mixture of clay–silt–gravel in which clay varied from 10 to 50% on weight basis. The transport rate of sediment is found to be higher in the initial period of time, however, it decreases with passage of time. Transport rate of sediment decreases with the increase in clay content, while it increases with excess shear stress. Bed degradation was found to be higher in upstream section than that of downstream section. Clay content affects the bed degradation profile as well as equilibrium time. Equilibrium time is found to be increased with clay content. The main parameters affecting the detachment and transport of sediment from cohesive bed are clay content, excess shear stress, and equilibrium time. Relationships have been developed for the computation of bed load transport rate, suspended load transport rate, and transient bed profile along with the auxiliary relationships for initial transport rate of sediment, equilibrium time and maximum degradation. All the developed relationships were found to be in good agreement with the observed ones.

Keywords Bed load · Clay–silt–gravel mixture · Cohesive bed · Sediment transport · Suspended load

Introduction

Transport of sediment in an alluvial channel occurs when shear stress developed on the channel bed due to flow exceeds a critical shear stress. Erosion appeared on the channel bed due to detachment of sediment when flow is sediment starved; however, deposition of sediment takes place when the sediment-carrying capacity of flow diminishes. The changes in sediment quantity may have a significant impact on a range of social, economic and environmental systems, such as collapse of structures like bridge, reservoir sedimentation, channel morphology, navigation system, flood problems, and aquatic habitat loss. Transport of sediment in a river may cause an issue in

water quality that may have a harmful impact on the aquatic environment, wild life, and human life. Owens et al. (2005) reported that 10% of lakes, rivers and bays of the USA have sediments contaminated with toxic chemicals. The processes controlling sediment transport are dynamic and highly variable and therefore understanding of sediment transport process greatly assists in proper functioning of river system and resolving the issues caused by sediment transport in the river domain. Fluvial sediment transportation is broadly divided into two distinct modes, i.e., bed load and suspended load. Bed load refers to sand grains, gravels, or larger particles that move along or near the channel bed by various mechanisms like traction and saltation. Suspended load refers to particles that are continuously entrained in the water column and mostly consist of fine sediments like clay and silt. Transport rate of sediment is much associated with the detachment of particles from the channel bed. The detachment of particles is associated with the flow characteristics along with the sediment properties. The sediment property of cohesive material is significantly different from that of cohesionless sediment (Mitchener and Torfs 1996). Li et al. (2018) conducted laboratory experiments to study the transport rate of cohesionless sediment of sand and

✉ Umesh K. Singh
umesh.ais@gmail.com

¹ Department of Civil Engineering, Indian Institute of Technology Roorkee, Roorkee, Uttarakhand 247667, India

² Present Address: Department of Civil Engineering, Global Institute of Management and Technology, Krishnanagar, Nadia, West Bengal 741102, India

gravel particles from a channel bed having uniform sand, uniform gravel, and sand–gravel mixture. They concluded that the transport rate is higher for gravel particles and slower for sand particles in sand–gravel mixture when compared to counterpart of uniform size due to the hide–exposure effect in non-uniform sediment. Shim and Duan (2017) conducted a laboratory experiment to measure bed load transport rate by manually collected data as well as using a series of images taken of moving particles by a high-speed camera. The study was for channel bed having cohesionless sediments. They concluded that the technique of high-speed camera could be successfully used for the measurement of bed load transport rate. Waters and Curran (2015) studied the morphological changes over channel bed made of sand–gravel mixture and sand–silt mixture in response to hydrograph flow by laboratory experiments. They concluded that sediment composition has a significant impact on channel bed morphology against higher hydrograph flow. They found that strong sand ripples in case of sand–silt mixture when compared to sand–gravel mixture against the same magnitude of hydrograph flow. When cohesionless sediment was mixed with cohesive sediment, the resulting mixture possesses a certain amount of cohesive property, therefore the mixture is treated as cohesive sediment mixture (Kothyari and Jain 2010). Several studies have been conducted for bed load and suspended load transport rate on cohesionless as well as cohesive bed like gravel bed, sand bed, gravel–sand mixture, clay–sand mixture and clay–gravel mixture (Paintal 1971; Proffitt and Sutherland 1983; Misri et al. 1984; Samaga et al. 1986; Woo et al. 1987; Swamee and Ojha 1991; Roberts et al. 1998; Wu et al. 2003; Aberle et al. 2004; Debnath et al. 2007; Jain and Kothyari 2009; Jepsen et al. 2010; Khullar et al. 2010; Houssais and Lajeunesse 2012; Wyss et al. 2016; Shim and Duan 2017). However, the presence of silt with gravel particles in cohesive mixture has not been studied so far and river bed materials often consist of a mixture of cohesive and cohesionless sediments. There is a need to explore different types of cohesive sediment mixtures, since the results of experimental study on sediment transport for one mixture may not be applicable to other mixtures. The present study focused on the development of a relationship for the computation of transport rate of sediment for the mixture of clay–silt–gravel in which the clay content varied from 10 to 50%. Further, the study was extended to develop the relationship for the computation of transient bed profiles.

Experimental setup and observations

The experiments were conducted in a tilting flume having 16 m length, 0.75 m width and 0.50 m depth in Hydraulic Engineering Laboratory, Civil Engineering Department, Indian Institute of Technology Roorkee, India. The channel had a test section of 6.0 m length, 0.75 m width and

0.18 m depth starting at a distance of 7.0 m from the channel entrance as shown by the schematic diagram of experimental flume in Fig. 1.

The flow in the flume was regulated with the help of a valve provided in the supply pipe connected to an overhead tank. The details about the experimental flume have been reported by Singh et al. (2017). The discharge measurement was done volumetrically through a tank provided at the end of the flume. A rectangular trap placed at the end of the flume just after the tail gate is used for the collection of bed load. The suspended load was collected through a depth-integrated sampler installed at the end of the flume just before the tail gate. A two-dimensional bed level profiler having the least count of 1.0 mm was used to measure the profile of the channel bed. The channel bed profile was also measured by a flat gauge of least count 0.10 mm. The water surface profile was measured with the help of a pointer gauge having the least count of 0.10 mm. Bed and water surface profile measurements were taken at longitudinal spacing of 0.50 m along the centre line of the flume.

Channel bed preparation

Clay, silt, and gravel with the median size (d_{50}) of 0.014 mm, 0.062 mm, and 5.50 mm and geometric standard deviation (σ_g) of 2.06, 1.18, and 1.31, respectively, were used in the present study. Clay used in the present study is classified as lean clay as per Unified Soil Classification System (ASTM D2487 2011). The σ_g was computed using $\frac{1}{2}[(d_{84}/d_{50}) + (d_{50}/d_{16})]$ where d_{84} , d_{50} and d_{16} are the sediment size such that 84%, 50% and 16% of material are finer than that size by dry weight, respectively (Garde and Ranga Raju 2000).

Clay–silt–gravel mixture was used for channel bed preparation in which clay content varied from 10 to 50% on weight basis, while silt and gravel were taken in equal proportions. Dried sediments were weighted as per proportion and then manually mixed together along with water as shown in Fig. 2. The prepared mixture was filled in the test section and compacted in three layers for preparing a cohesive bed (Ahmad et al. 2018). In this, each layer was compacted with a cylindrical roller having weight equal to 400 N. Figure 2 shows the preparation of sediment mixture and compaction of channel bed using cylindrical roller. The sides of channel bed were compacted using hand rammer having a rectangular bottom. Details about bed preparation have been reported by Ahmad et al. (2018). Samples were taken out from the downstream section of prepared cohesive bed for the determination of their bulk density, unconfined compressive strength, and moisture content. The bulk unit weight of sediment mixture was determined using standard core cutter method as per IS-2720 Part XXIX (Bureau of Indian Standards (IS) 1975). Unconfined compressive strength

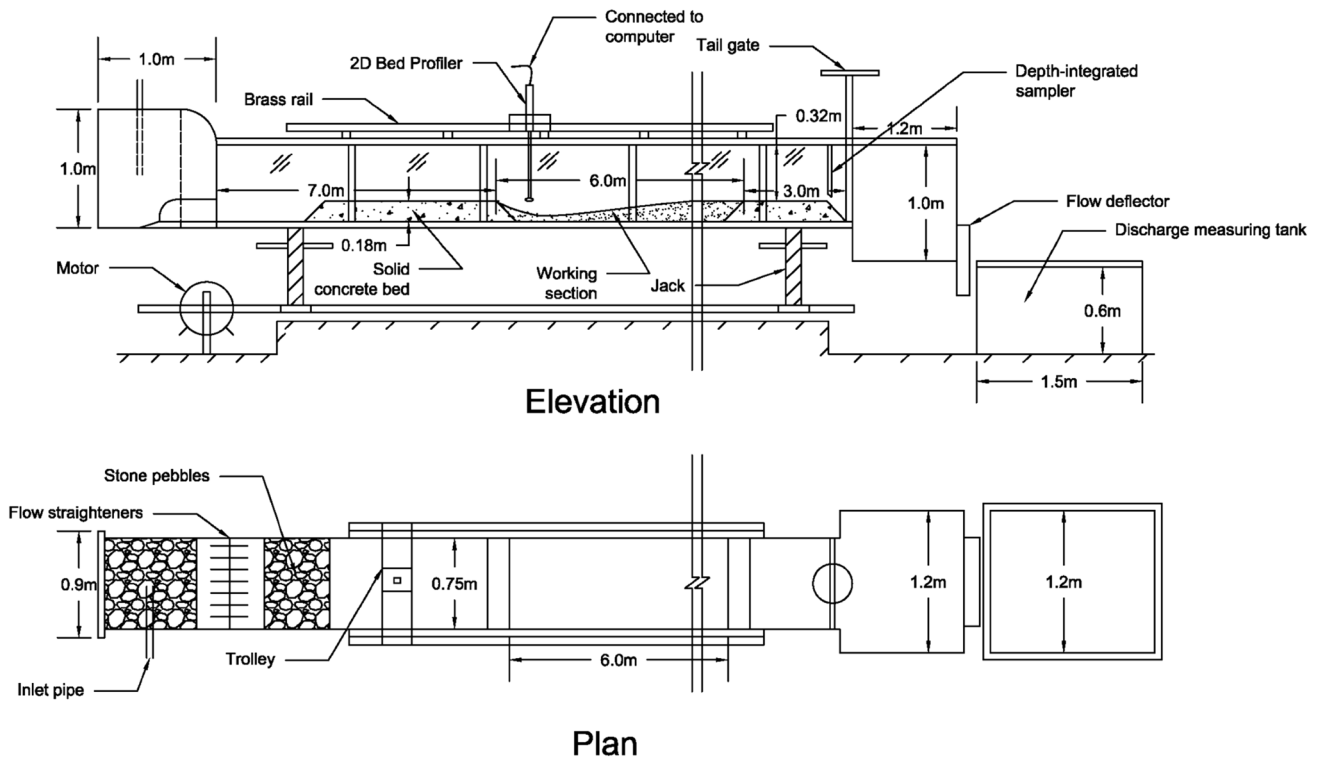


Fig. 1 Schematic diagram of flume



Fig. 2 Preparation of sediment mixture and channel bed

(UCS) was determined in laboratory as per IS-2720 Part X (Bureau of Indian Standards (IS) 1991). Water content was determined as per the dry oven method for the compacted cohesive bed corresponding to all runs. Dry density of the channel bed was computed using determined value of bulk

density and water content of the bed. The void ratio of the channel bed was determined using the computed value of dry density.

Experimental procedure

Experiments were conducted on a combination of two bed slopes (i.e., $S_0=0.00721$ and 0.00946) and two discharges ($Q=0.05$ m³/s and 0.07 m³/s). Incoming flow was allowed in the flume at the desired bed slope and discharge. Measurements for bed profile, water surface profile, bed load, and suspended load were taken at different time intervals. Initially, the time interval for measurements for bed profile, water surface profile, etc., was kept as 15 min, as the transport rate of sediment was observed to be high while later on this time interval was increased to 30, 45, 60, 120 min as transport rate slowed down with the passage of time. The duration of each run was counted till the bed profile seems to be in a static condition and very less or no sediment transport was occurring.

The coarse sediment gravel was transported as bed load and collected in a trap placed at the end of the flume just after the tail gate. The collected sediment in the trap was dried and weighted. Bed load transport rate was computed as the measured bed load per unit channel width per unit time (Garde and Ranga Raju 2000). The suspended load was collected through a depth-integrated sampler installed at the end of the flume just before the tail gate. The fine particles, clay and silt, were detached from the channel bed and transported as suspended load. The suspended sediments in the form of sediment-laden water were collected in a 15 L capacity bucket by traversing the depth-integrated sampler over the entire width of flow (Jain and Kothiyari 2010). The collected sediment-laden water in the bucket was weighted and left for over 24 h so that the suspended sediment was settled down at the bottom of the bucket. After settlement of fine sediments, the water was removed from the bucket and the wetted sediment at the bottom of the bucket was transferred to the pan and placed in oven for drying. The dried suspended sediment was weighted and concentration of suspended load was computed by dividing the weight of dry sediment with the measured weight of sediment-laden water (Garde and Ranga Raju 2000).

Results and discussion

Sediment load transport

The present study carried out the experimental study in which gravel particles moved as bed load and clay–silt particles as suspended load in clay–silt–gravel mixture. In case of cohesive mixture, the transport rate of bed load and suspended load depends on various factors like clay percentage, sediment size, and shear stress. In view of this, the variation of transport rate of gravel particles with clay percentage, time, and excess shear stress has been shown in

Figs. 3a, b, 4a, b, and 5a, b, respectively. Figure 3a, b shows the influence of clay content on transport rate of bed load and suspended load at time $t=30$ min for all flow conditions. Figure 3a reveals that the transport rate of bed load decreases with the increase in the clay percentage for the cohesive mixture of clay–silt–gravel. The increase in the clay percentage in the sediment mixture increases the influence of cohesion which leads to a stronger bond among the particles and resulted in a low transport rate. A similar trend has been found for the suspended load as illustrated in Fig. 3b.

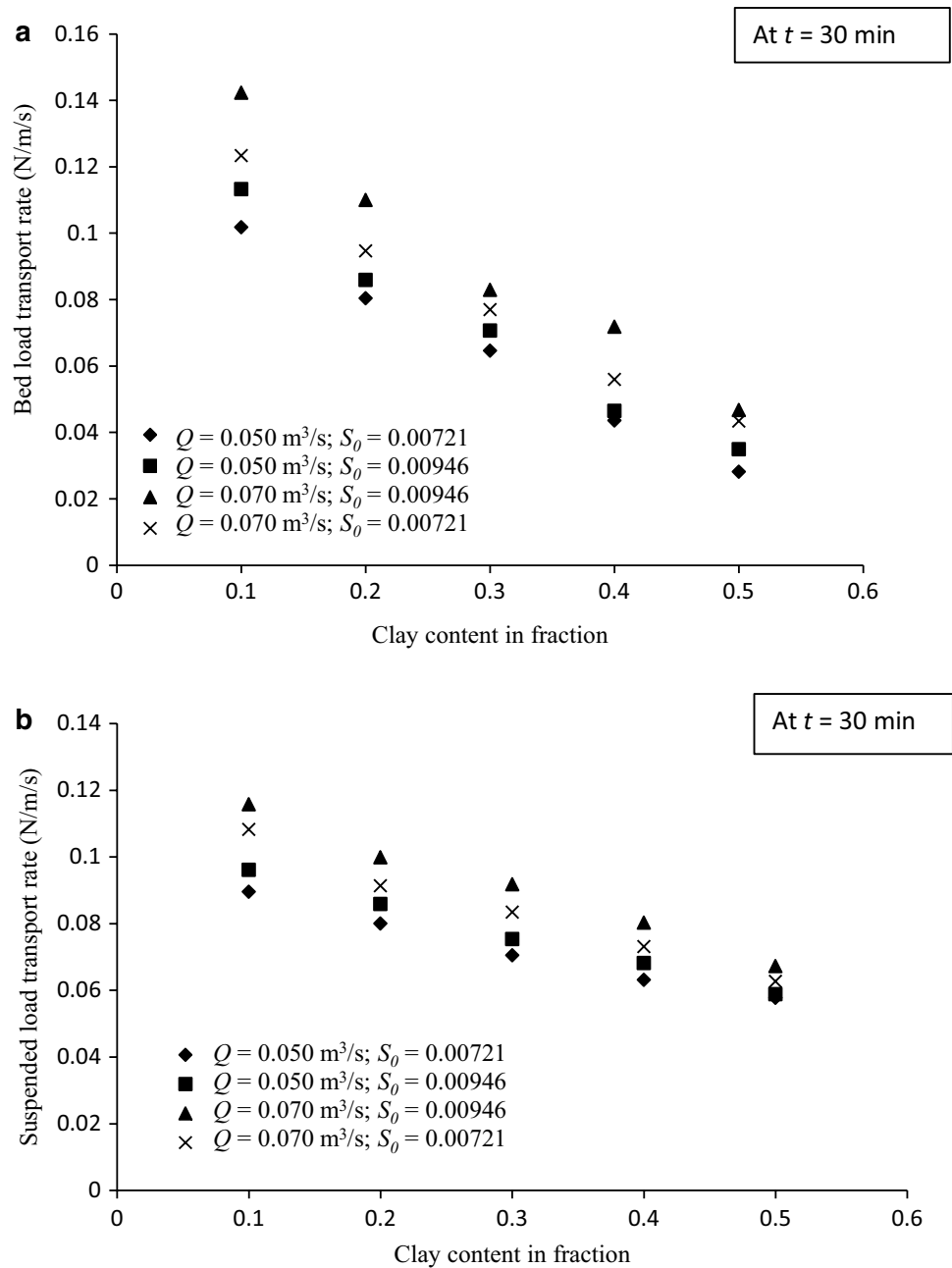
It was noticed that bed load and suspended load transport rate decrease with time passage. Since transport of sediment from the channel bed resulted in bed degradation and bed degradation allows higher depth of flow which leads to low shear stress on the channel bed, it may cause a low transport rate with the passage of time. The variation of bed load and suspended load transport rate against time has been illustrated in Fig. 4a, b, respectively, which show that transport rate decreases with time for the clay content in the mixture.

Figure 5a, b shows the plot of transport rate of bed load and suspended load with excess shear stress, respectively, at time $t=30$ min for all the flow conditions. The transport rate of sediment increases with the increase in excess shear stress as illustrated in Fig. 5a, b which may be attributed to higher shear stress corresponding to high excess shear stress that allows high energy to flow and that results in high transport rate of sediment.

It can be seen from Fig. 4a, b that the transport rate of sediment decreases with the increase in time, i.e., the transport rate is higher in the initial period of time. Transport rate in the initial period of time is considered as the initial transport rate of sediment which is taken as corresponding to the first 15 min of the start of experimental run, i.e., first 15 min from the start of erosion process. The initial transport rate of sediment is an important aspect in sediment transport study, as a higher initial transport rate may lead to higher degradation in the channel bed. Hence, the transport rate of sediment with passage of time depends on the initial transport rate of sediment. The initial bed load transport rate is influenced by the cohesion, so it varied with the clay percentage in the sediment mixture. Initial bed load transport rate is found to decrease with the increase in clay percentage for the cohesive mixture of clay–silt–gravel. A higher percentage of clay in the mixture binds the particles together more tightly and that responded to a decrease in initial bed load transport with the increase in clay percentage. A similar trend has been found for the initial suspended load transport rate which is illustrated in Fig. 6.

The total time taken in the experimental run, i.e., from start of the erosion to reach the equilibrium condition is considered as equilibrium time. The condition is treated as equilibrium condition when changes in bed level with time are negligible and sediment transport rate becomes negligible,

Fig. 3 a Variation of bed load transport rate with clay fraction, **b** variation of suspended load transport rate with clay fraction



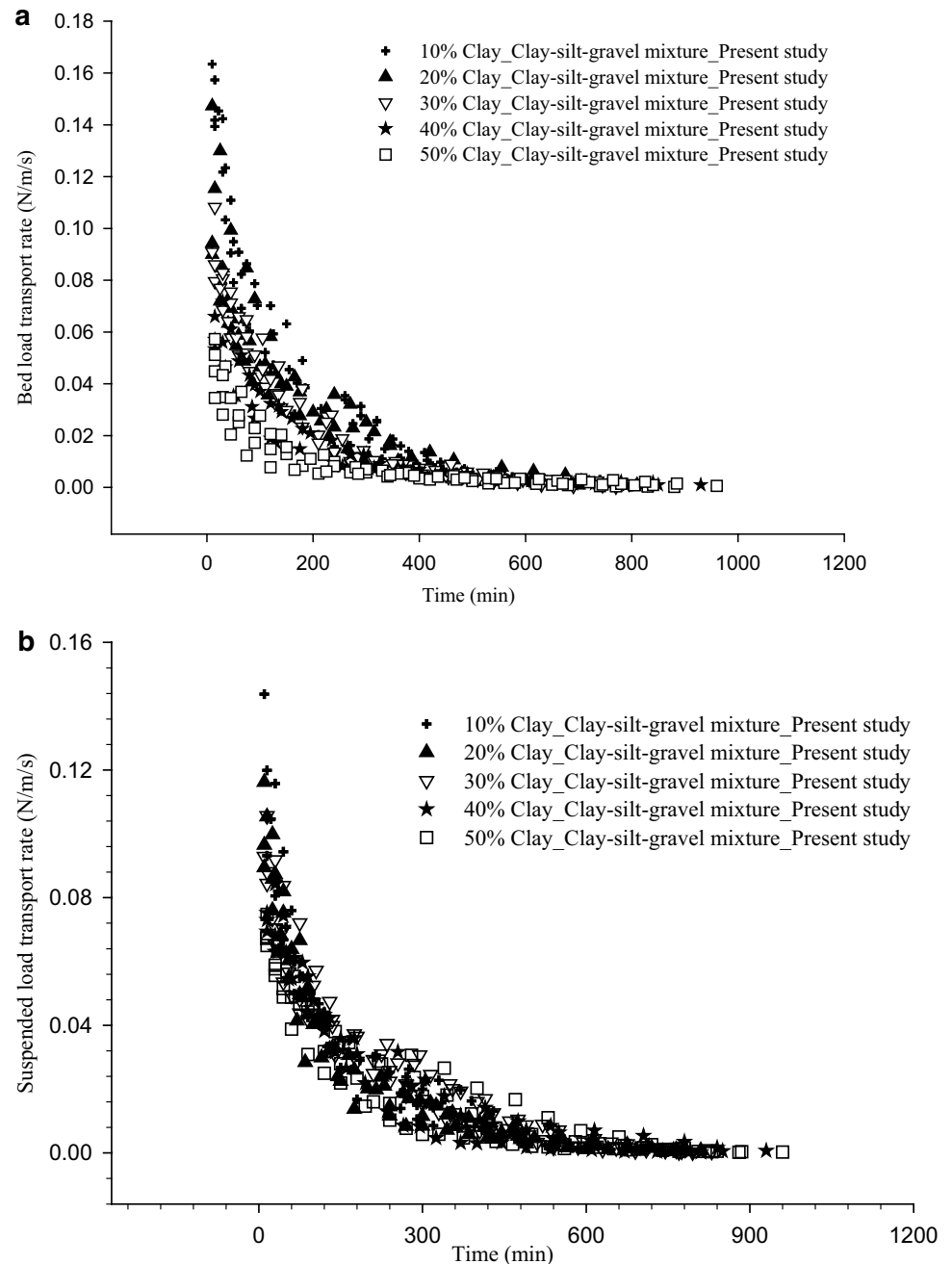
i.e., transport rate of sediment reaches to less than 2% of initial transport rate. Equilibrium time is considered here as one of the parameters that may influence the transport rate of sediment. Equilibrium time is found to vary with the clay content in the mixture. It is observed that the equilibrium time increases with the increase in clay percentage as illustrated in Fig. 7.

Degradation and bed profiles

The transient bed profiles were measured at mid of the flume width at a longitudinal interval of 0.50 m along the flow

direction for all experimental runs. Bed degradation was found to be more in the upstream section than that of downstream section for all clay content in the mixture. In view of this, a plot is made as shown in Fig. 8 that shows the amount of degradation that occurred on the channel bed at $t = 75 \text{ min}$ for 20% clay content in the clay–silt–gravel mixture. High degradation in the upstream section may be attributed to the higher energy associated with flow when it interacts with the mobile interface, however, energy decreases due to the sediment being carried with the flow as the flow moved forward. Figure 8 reveals that maximum degradation occurred at 50 cm distance from the entrance of upstream working

Fig. 4 **a** Bed load transport rate against time, **b** suspended load transport rate against time



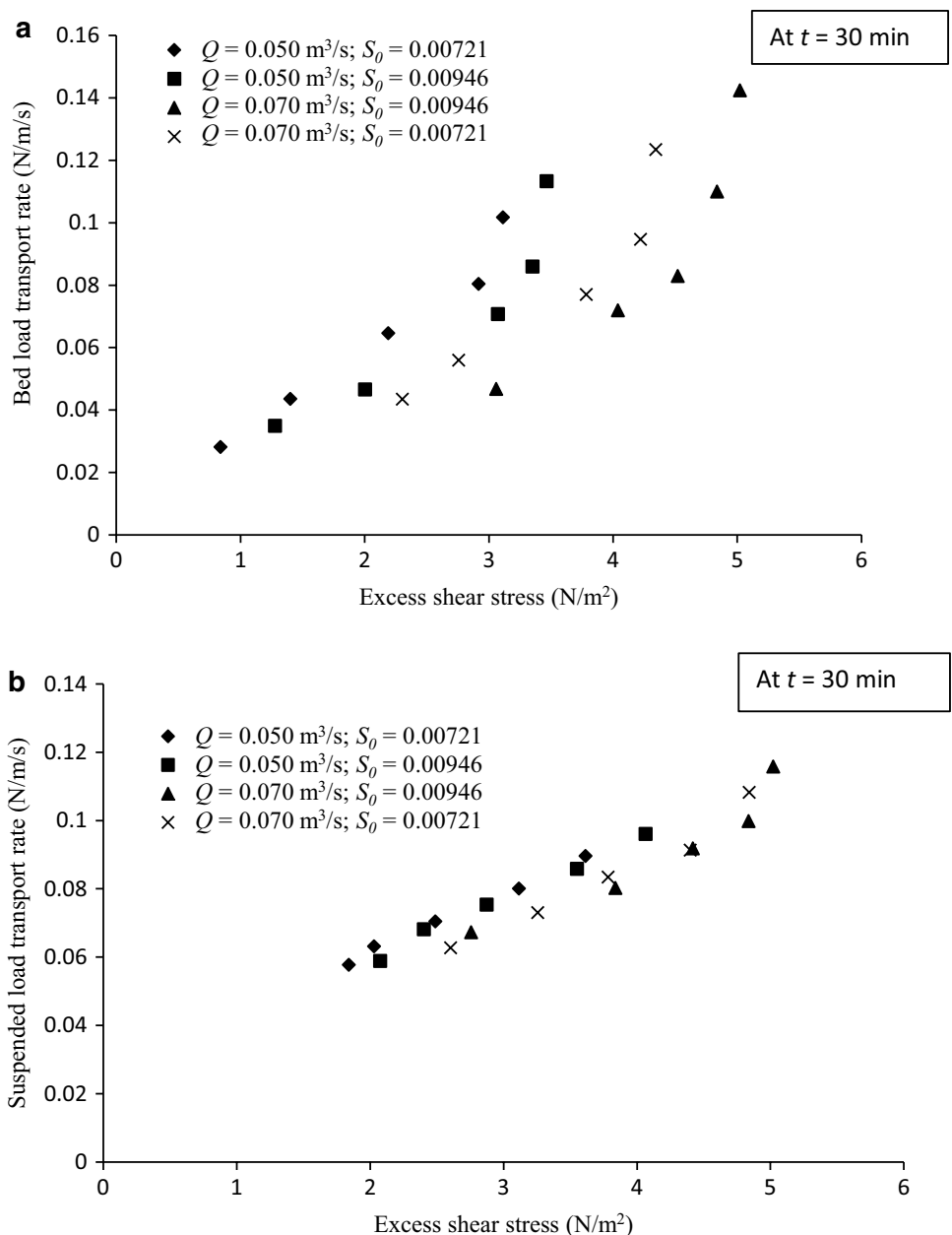
section. The bed profile of the channel bed varied with the clay percentage in the sediment mixture as well as with the excess shear stress. Figure 9 shows the effect of clay content on degradation of channel bed at channel section $X=0.5$ m and $t=30$ min for all the flow conditions. Figure 9 reveals that the degradation of channel bed decreases with the increase in clay percentage. Bed degradation on channel bed at a section $X=1.0$ m for 20% clay content is plotted with time as illustrated in Fig. 10 which shows that the bed degradation at that section increases with the passage of time.

Development of relationship for sediment transport

Relationship development for transport rate

Relationships have been developed in the present study for the computation of the bed load and suspended load transport rate along with the transient bed profile for the cohesive mixture of clay–silt–gravel. Range of the measured parameters for bed load and suspended load is given in Table 1.

Fig. 5 a Variation of bed load transport rate with excess shear stress, **b** variation of suspended load transport rate with excess shear stress



The following parameters have been considered for the development of relationship for the computation of bed load transport rate of sediment:

$$q_{BT} = f(t, t_e, q_{BT}^i) \tag{1}$$

Here q_{BT} is the bed load transport rate (N/m/s); t is time (s), t_e is equilibrium time (s), and q_{BT}^i is the initial bed load transport rate (N/m/s).

Equation (1) may be written in the dimensionless form as shown below:

$$q_{BT}^* = f\left(\frac{t}{t_e}\right) \tag{2}$$

Here q_{BT}^* is the dimensionless bed load transport rate and computed as:

$$q_{BT}^* = \frac{q_{BT}}{q_{BT}^i} \tag{3}$$

Equation (2) represents the functional relationship for the dimensionless bed load transport rate. The plot has been made between the observed dimensionless bed load transport rate and functional parameter of $\frac{t}{t_e}$ and a curve is fitted between them. The fitted curve is illustrated in Fig. 11 for the cohesive sediment mixture of clay–silt–gravel and the

Fig. 6 Variation of initial suspended load transport rate with clay fraction

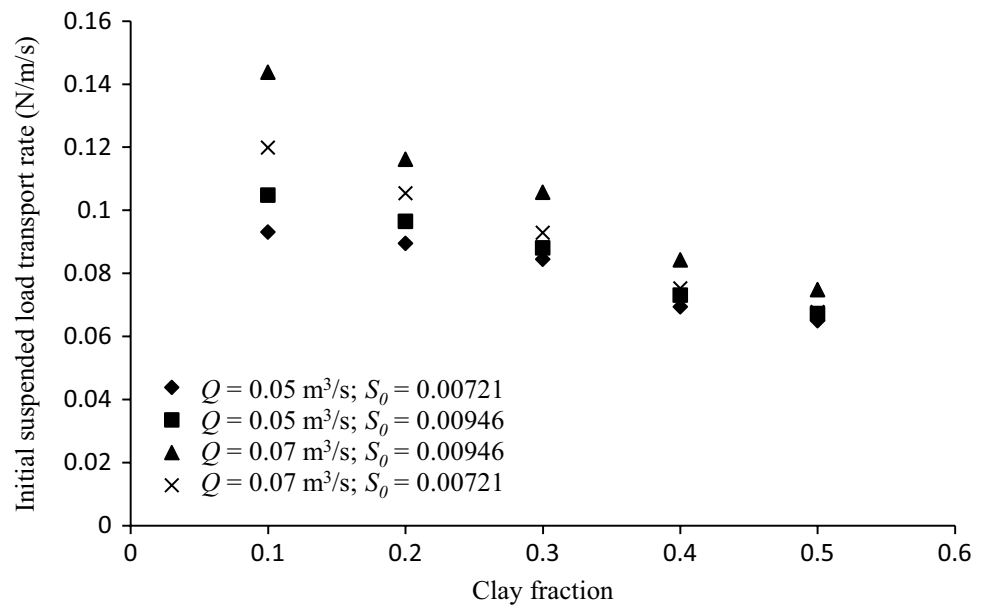
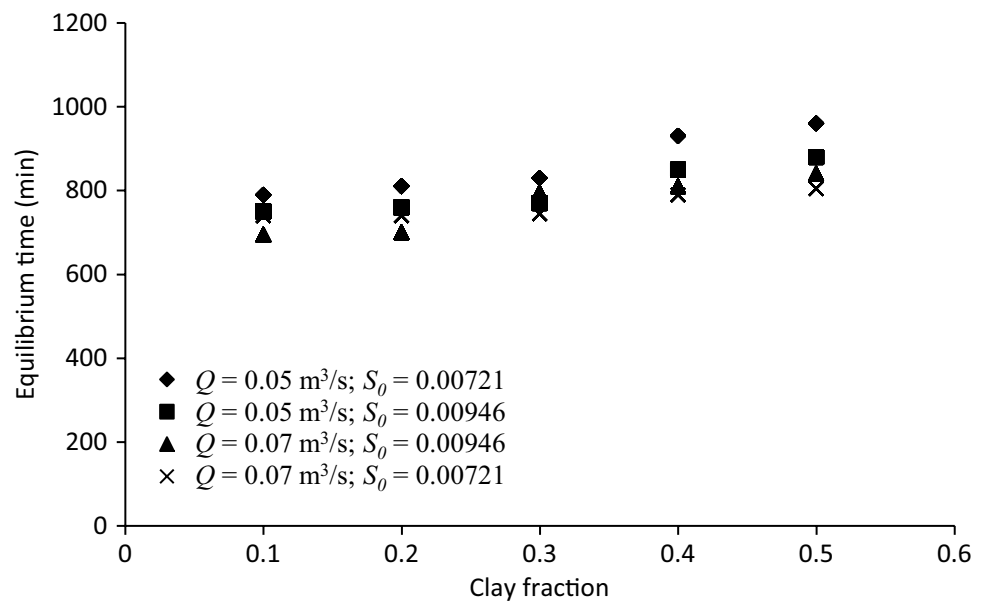


Fig. 7 Equilibrium time with clay percentage for clay–silt–gravel mixture



corresponding formulation from the fitted curve has been represented by Eq. (4) as shown below:

$$q_{BT}^* = 1 - 0.97 \left[1 - e^{-6.089 \left(\frac{t}{t_c} \right)} \right] \tag{4}$$

Similarly in case of suspended load transport rate, the curve was fitted as illustrated in Fig. 12 and correspondingly a relationship has been proposed for the computation of suspended load transport rate.

In Fig. 12, q_{sf}^* is the dimensionless suspended load transport rate and computed as: $q_{sf}^* = \frac{q_{sf}}{q_{sf}^i}$, where q_{sf} is the sus-

pended load transport rate (N/m/s), and q_{sf}^i is the initial suspended load transport rate (N/m/s).

$$q_{sf}^* = 1 - 0.365 \left[1 - e^{-1.134 \left(\frac{t}{t_c} \right)} \right] - 0.754 \left[1 - e^{-6.97 \left(\frac{t}{t_c} \right)} \right] \tag{5}$$

A plot has been prepared between the observed and computed value of dimensionless bed load and suspended load transport rate and a regression analysis was done which shows a good regression coefficient as illustrated in Figs. 13 and 14, respectively.

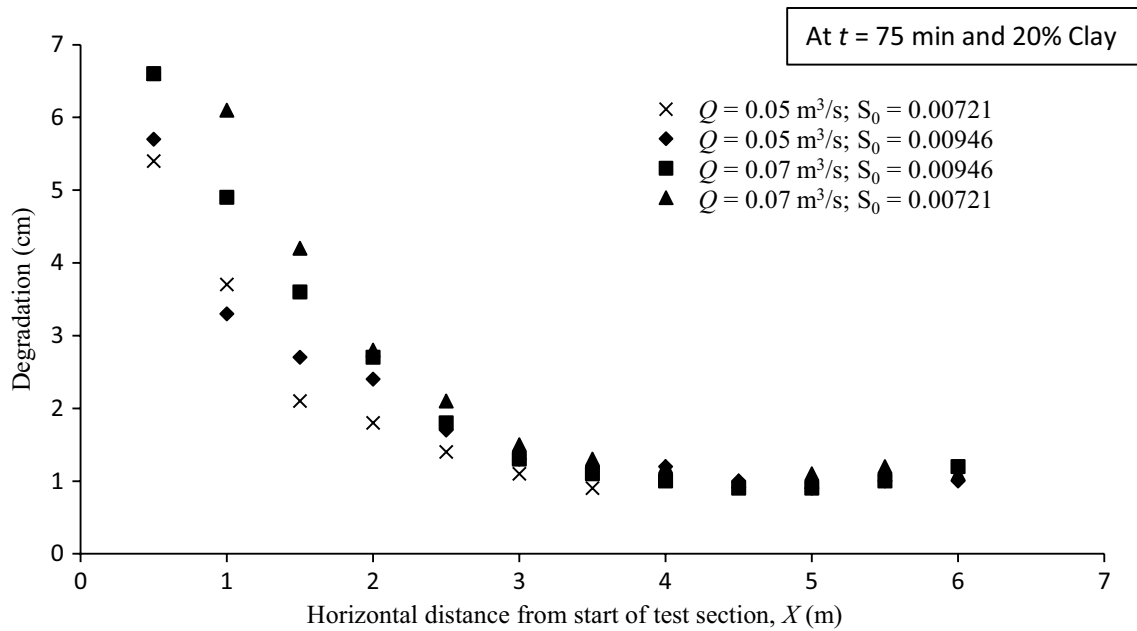


Fig. 8 Bed degradation along the channel bed

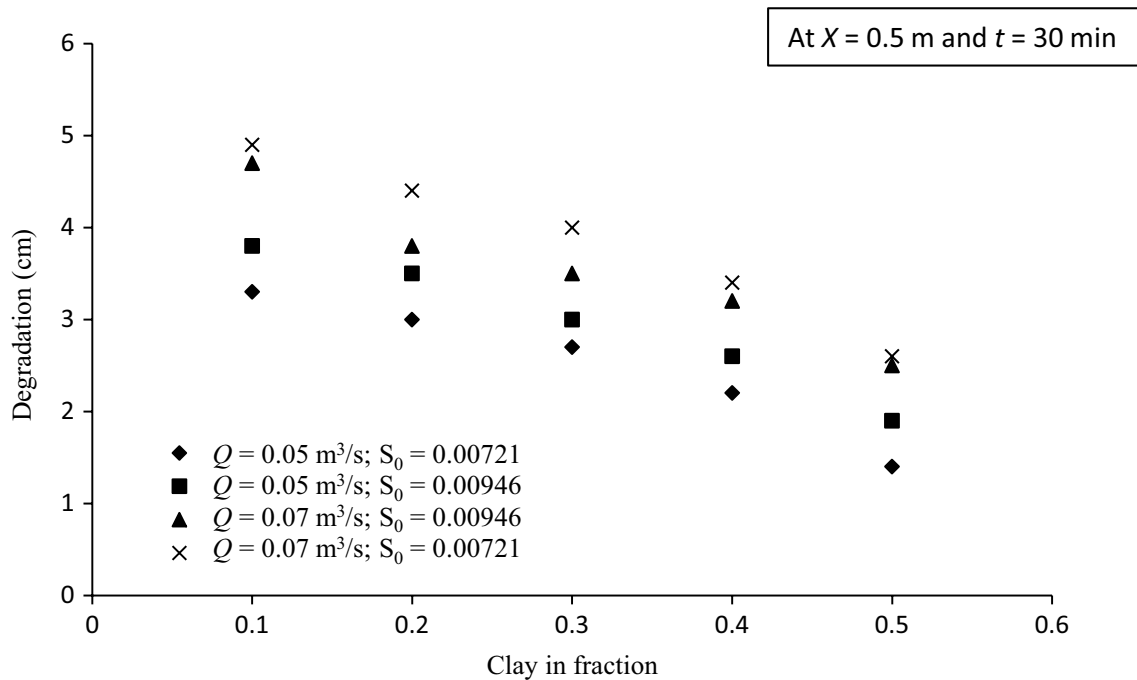


Fig. 9 Bed degradation with clay fraction

To get the transport rate of sediment, relationships are needed for the computation of initial transport rate and equilibrium time. The initial transport rate may be expressed as:

$$q_{BT}^i = f(P_c, \tau, \tau_{cc}, \rho, \rho_s, d_a, g, v) \tag{6}$$

Here P_c is the clay percentage in fraction, τ is the shear stress (N/m²) developed due to the incoming flow, τ_{cc} is the critical shear stress (N/m²) for cohesive sediment mixture, ρ_s and ρ are particle and fluid densities (Kg/m³), respectively, d_a is arithmetic mean size (m) of the cohesive sediment mixture,

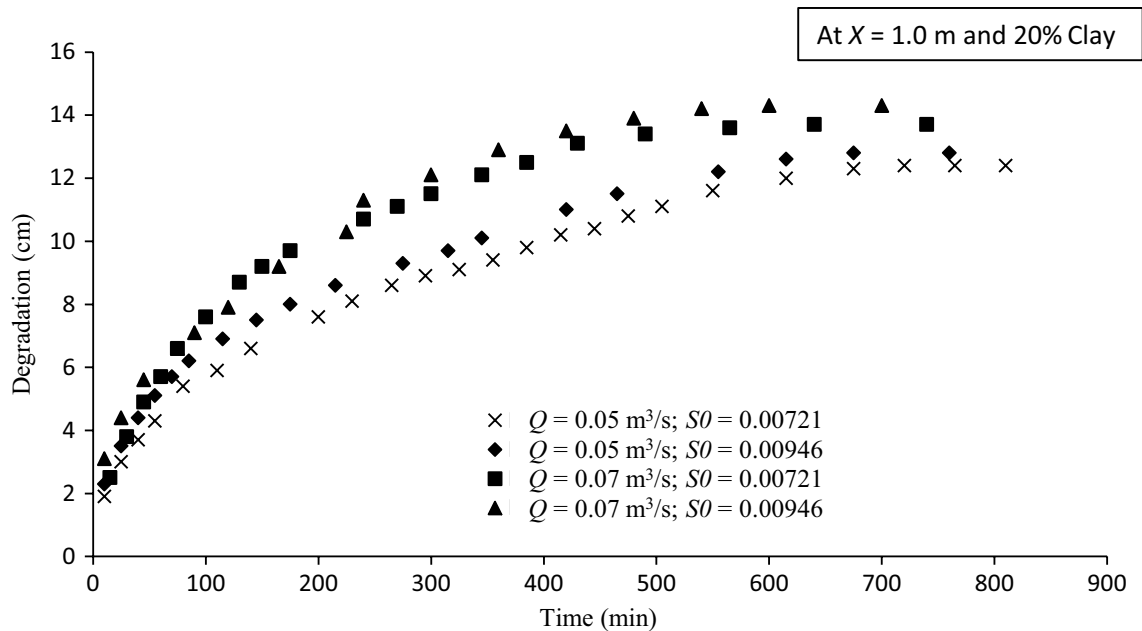


Fig. 10 Bed degradation with time

g is gravitational acceleration (m/s^2), and ν is the kinematic viscosity of fluid (m^2/s).

Equation (6) may be written in the dimensionless form as below:

$$q_{BT}^{i*} = f(P_c, \tau_e^*) \tag{7}$$

Here q_{BT}^{i*} is the dimensionless initial bed load transport rate and expressed as:

$$q_{BT}^{i*} = \frac{q_{BT}^i}{(\rho_s - \rho)g\nu} \tag{8}$$

τ_e^* is the dimensionless excess shear stress and expressed as:

$$\tau_e^* = \frac{\tau - \tau_{cc}}{(\rho_s - \rho)gd_a} \tag{9}$$

Shear stress due to incoming flow (τ) was measured before the start of working section. Shear stress (τ) was determined as $\rho g R S_0$ (usual notation) with easily measurable parameters.

Critical shear stress (τ_{cc}) can be determined using the proposed formula by Ahmad et al. (2018) for the clay–silt–gravel mixture which is given below as:

$$\frac{\tau_{cc}}{\tau_{cm}} = 1 + 0.354 P_c^{2.081} (1 + P_s)^{2.275} \left(\frac{\rho_b}{\rho} \right)^{4.10}.$$

Here τ_{cm} is critical shear stress (N/m^2) for the cohesionless sediment having sediment size as arithmetic mean of

sediment mixture, P_s is the silt content in fraction, and ρ_b is the bulk density (kg/m^3) of the cohesive sediment mixture.

τ_{cm} can be computed as per Brownlie’s (1981) equation which represents the revised Shields curve (Ahmad et al. 2018).

Shear stress indicates the total shear stress with which incoming flow is likely to strike on cohesive bed of working section. However, cohesive bed resists the flow as per its critical shear stress value which varied as per clay content. Hence, the difference between shear stress and critical shear stress responds to transport of bed load which is termed here as excess shear stress.

The gravel particle was transported as bed load and collected in a trap placed at the end of the flume just after the tail gate. The trap was rectangular in shape and it was made of a wire mess supported on the iron rod. It was covered with a net cloth such that bed load sediments were retained on the trap. The collected sediment in the trap was dried and weighted. The bed load was measured at regular time intervals during the experiments. Initially, the time interval for measurements was kept at 15 min, as the transport rate of sediment was observed to be faster while later on this time interval was increased to 30, 45, 60, 120 min as the transport rate decreased with passage of time. The duration of each run was continued till the bed profile seems to be in static condition, i.e., very less or no sediment transport was occurring.

After a large number of trials, the following relationship is proposed for the computation of q_{BT}^{i*} for the cohesive

Table 1 Range of data on erosion and transport for clay-silt-gravel mixture

Mixture	P_c (%)	d_a (m)	UCS (kN/m ²)	Q (m ³ /s)	S_0 (-)	t_e (min)	q_{BT}^i (N/m/s)	q_{sf}^i (N/m/s)	q_{BT}^* (N/m/s)	q_{sf}^* (N/m/s)
Clay-silt-gravel	10–50	0.0013975–0.0025043	0.00000–42.17261	0.05010–0.07022	0.00721–0.00946	695–960	0.03457–0.16345	0.06502–0.14376	0.000233–0.163456	0.000262–0.143767

sediment mixture in the present study using the least squares technique.

$$q_{BT}^{i*} = 25.446(1 + P_c)^{-3.36} (\tau_c^*)^{0.298} \tag{10}$$

Similarly, a relationship has been proposed for the computation of dimensionless initial suspended load transport rate (q_{sf}^{i*}) for the clay-silt-gravel mixture as follows:

$$q_{sf}^{i*} = 12.018(1 + P_c)^{-1.517} (\tau_c^*)^{0.161} \tag{11}$$

The computed value of q_{BT}^{i*} and q_{sf}^{i*} from Eqs. (10) and (11) shows a good agreement with the observed data as illustrated in Figs. 15 and 16, respectively.

The following parameters have been considered in the development of relationship for equilibrium time.

$$t_e = f(P_c, \tau, \tau_{cc}, \rho, \rho_s, d_a, g) \tag{12}$$

Equation (12) can be represented in the dimensionless form using the dimensional analysis as shown below:

$$t_e^* = f(P_c, \tau_c^*) \tag{13}$$

Here t_e^* is the dimensionless equilibrium time and is expressed as:

$$t_e^* = \left(\sqrt{\frac{gt_e^2}{(S-1)d_a}} \right)^{1/7} \tag{14}$$

Here

$$S = \frac{\rho_s - \rho}{\rho} \tag{15}$$

P_c has been taken in account to consider the effect of various percentage of clay, while the parameter τ_c^* accounts for the sediment transport phenomena. After a large number of trials, the following relationships are proposed for the computation of t_e^* for the cohesive sediment mixture.

$$t_e^* = 7.668(1 + P_c)^{0.197} (\tau_c^*)^{-0.011} \tag{16}$$

Equation (16) represents the relationship for the computation of t_e^* for the cohesive sediment mixture of clay-silt-gravel based on the present study data as the other investigators' data were not available. The computed value of t_e^* from Eq. (16) shows a good agreement with the observed data as illustrated in Fig. 17.

Relationship development for bed profiles

Degradation in the channel bed starts when the developed shear stress on the channel bed is sufficiently large enough to mobilize and transport the bed particles and this degradation continues till a stable bed condition is reached. The transient

Fig. 11 Fitted curve for bed load transport rate

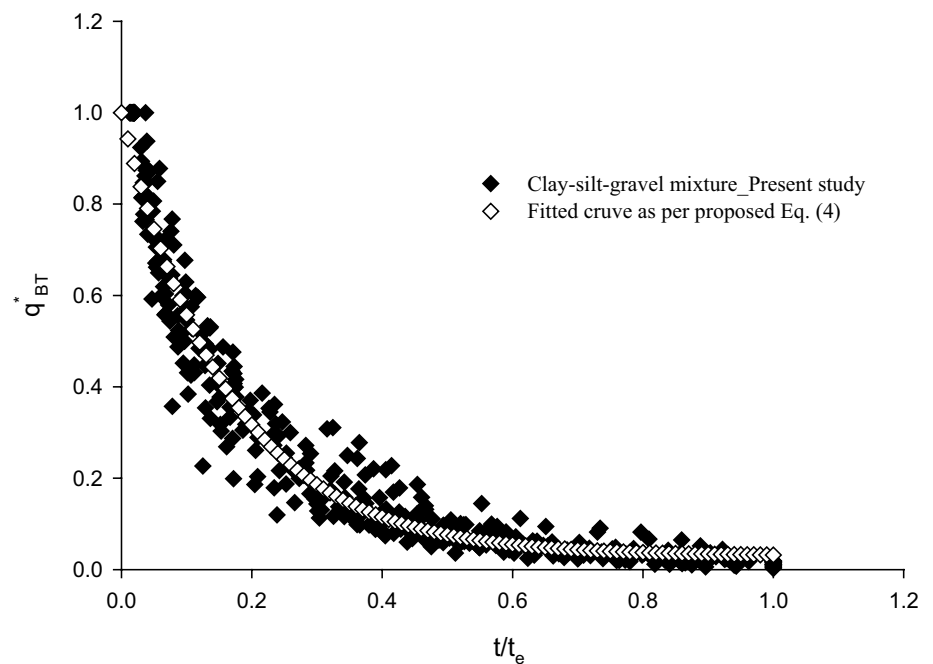
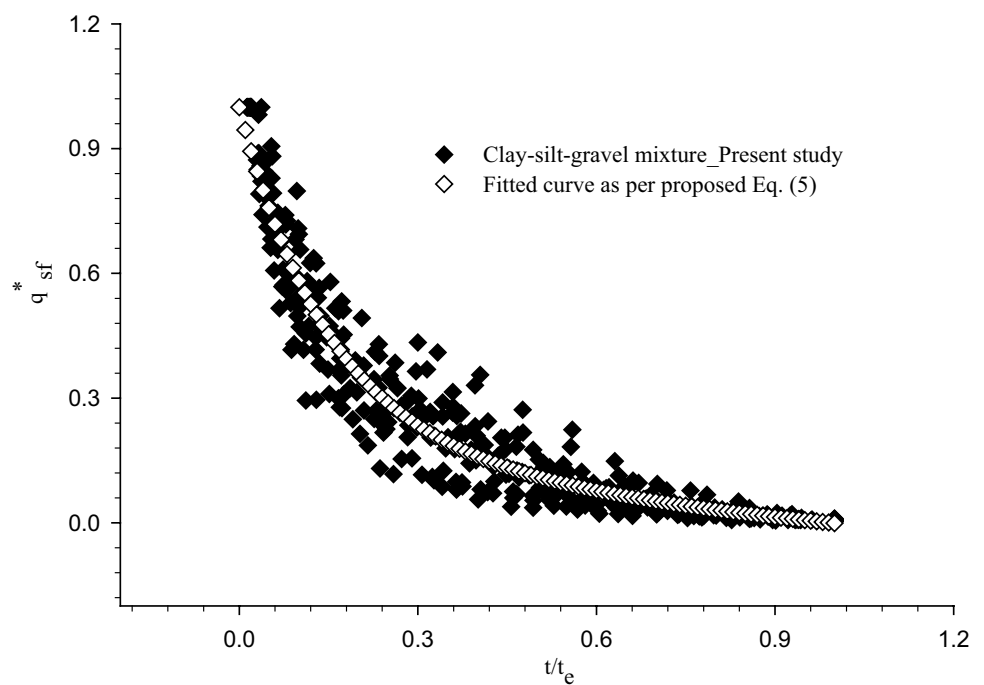


Fig. 12 Fitted curve for suspended load transport rate



bed profiles were measured at the mid of flume width at a longitudinal interval of 50 cm along the flow direction. Degradation from the channel bed is higher initially and then decreases with passage of time, consequently degradation is higher initially. Bed profiles of channel bed with passage of time have been plotted with reference to zero degradation indicated by initial bed level as illustrated in Fig. 18. Figure 18 reveals that the degradation is high in upstream section of channel bed than that of downstream. Bed profile

was getting stabilized towards the end of run, as nearly the same bed profiles were observed towards the end of run time as shown in Fig. 18. Physical appearance of the channel bed was visualized at the end of run which supports higher degradation in upstream section of the channel bed as illustrated in Fig. 19. Figure 19 shows the degradation profile for 50% of clay content in clay-silt-gravel mixture at discharge and bed slope of $0.05 \text{ m}^3/\text{s}$ and 0.00946 , respectively.

Fig. 13 Comparison between computed and observed value of q_{BT}^*

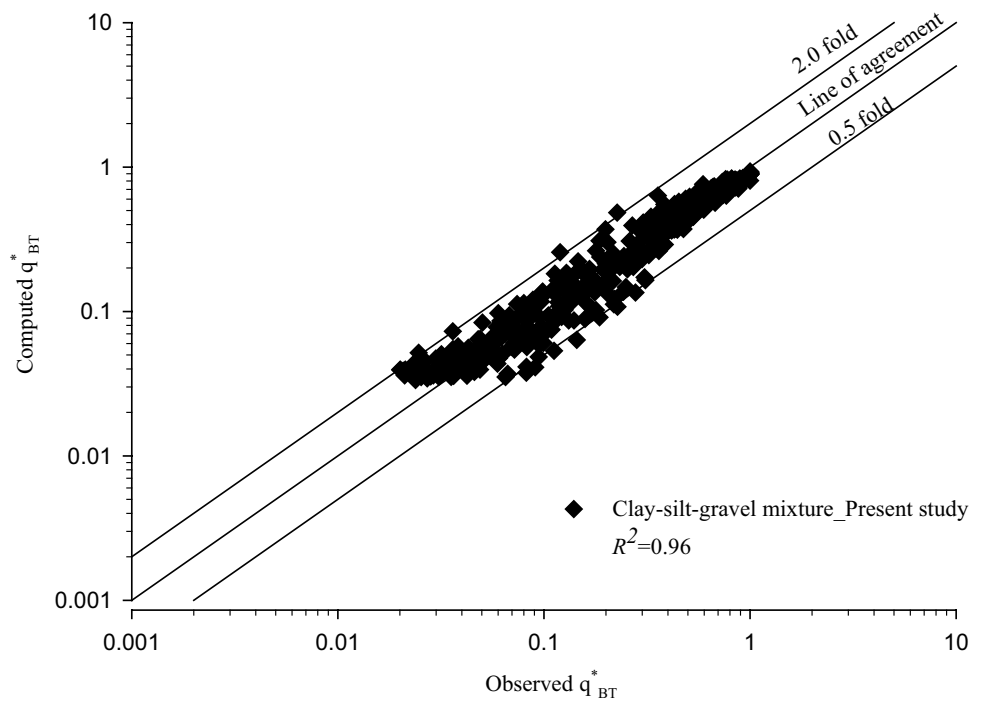
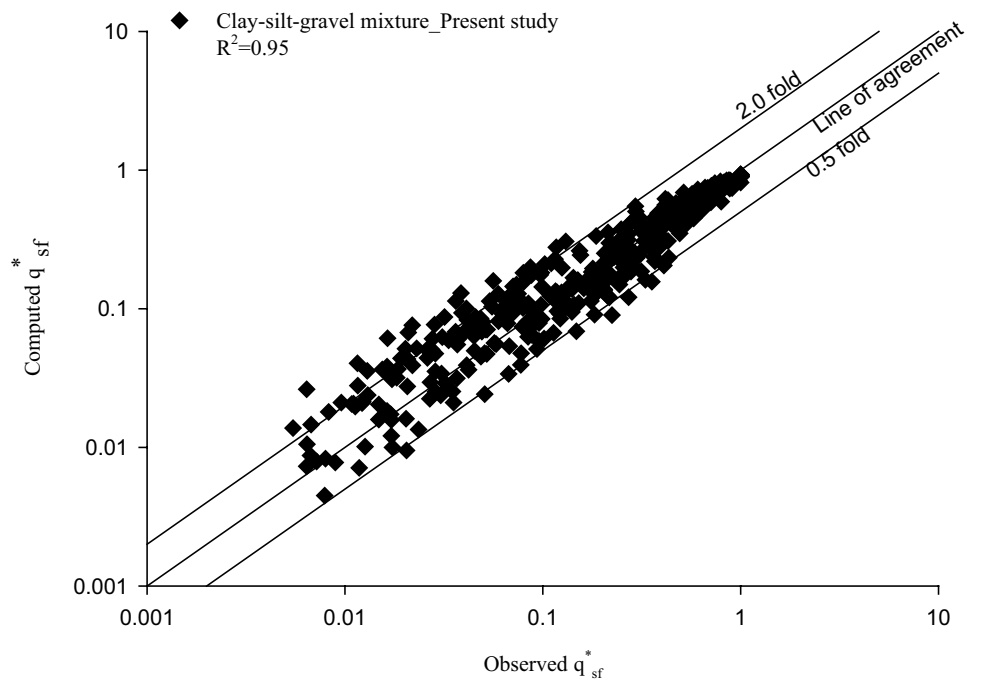


Fig. 14 Comparison between computed and observed value of q_{sf}^*



Various parameters have been considered in the present study to develop a relationship for the computation of bed profile for the cohesive sediment mixture of clay–silt–gravel. The functional relationship may be written as:

$$z = f(z_{max}, t, t_e, X, L_{max}) \tag{17}$$

Here z is bed degradation (m), z_{max} is the maximum degradation in the test section of channel bed (m), X is the horizontal distance in longitudinal direction from start of test section (m), and L_{max} is distance from start of test section where maximum degradation occurs (m).

Before the development of a relationship for the computation of bed degradation, the formulation has to be made for the computation of maximum degradation (z_{max}) in the

Fig. 15 Comparison between computed and observed value of q_{BT}^{i*}

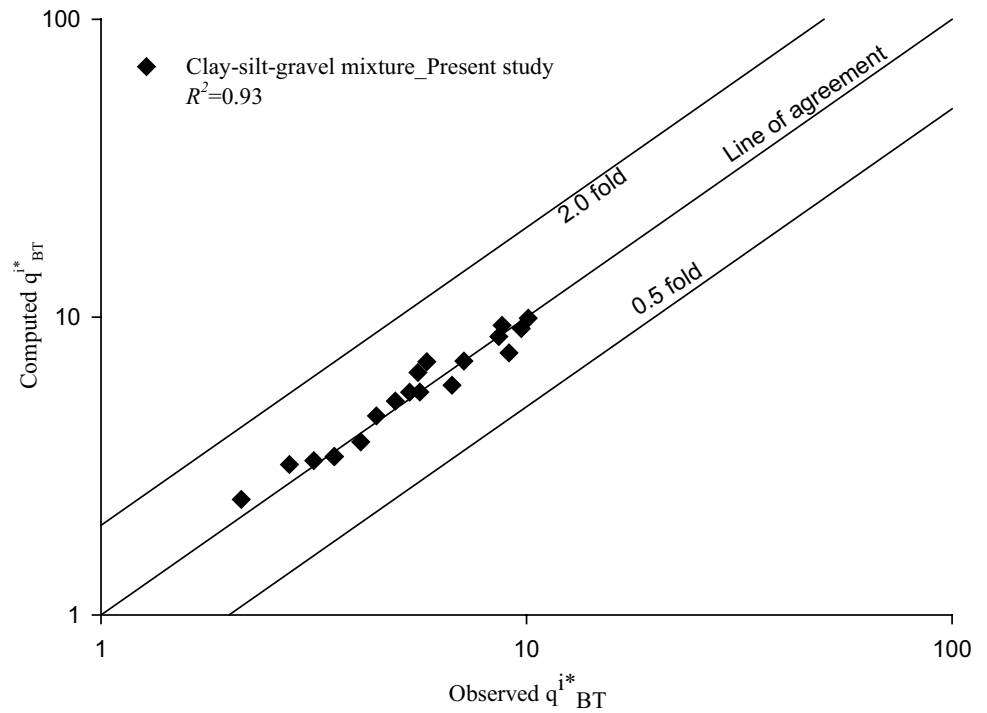
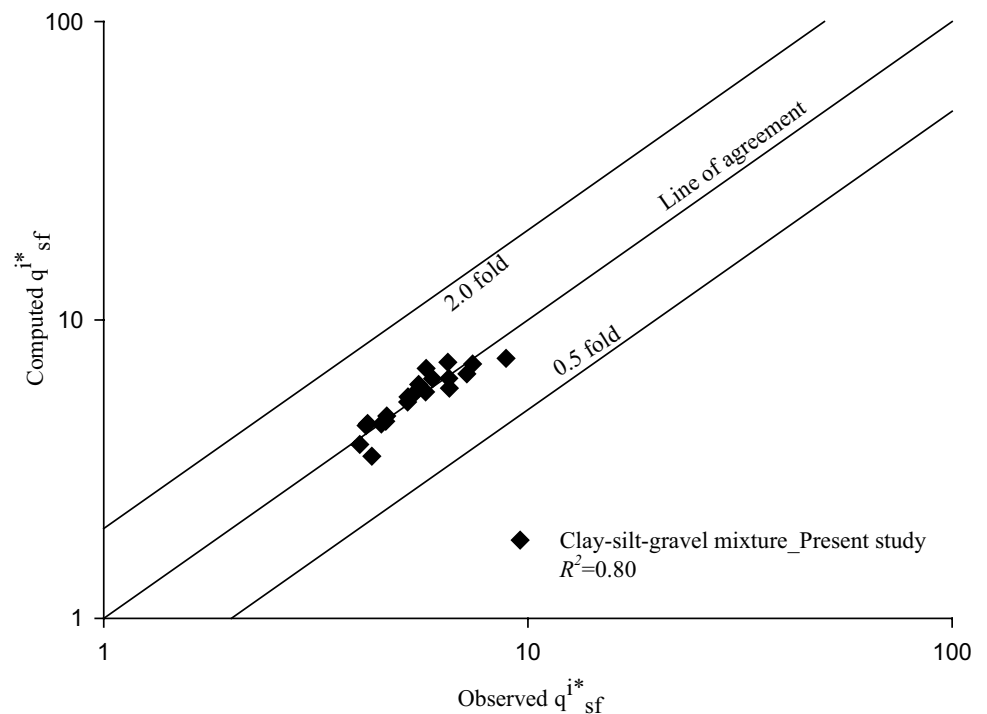


Fig. 16 Comparison between computed and observed value of q_{sf}^{i*}



cohesive channel bed which has been developed as below. The functional relationship for maximum degradation (z_{max}) may be written as:

$$z_{max} = f(P_c, \tau_e, \rho_s, \rho, g, d_a, q)$$

Here q is discharge per unit width (m^2/s).

The functional form of Eq. (18) can be presented in the dimensionless form as shown below:

$$\frac{z_{max}}{\left(\frac{q^2}{g}\right)^{1/3}} = f(P_c, \tau_e^*) \tag{19}$$

Fig. 17 Comparison between computed and observed dimensionless equilibrium time

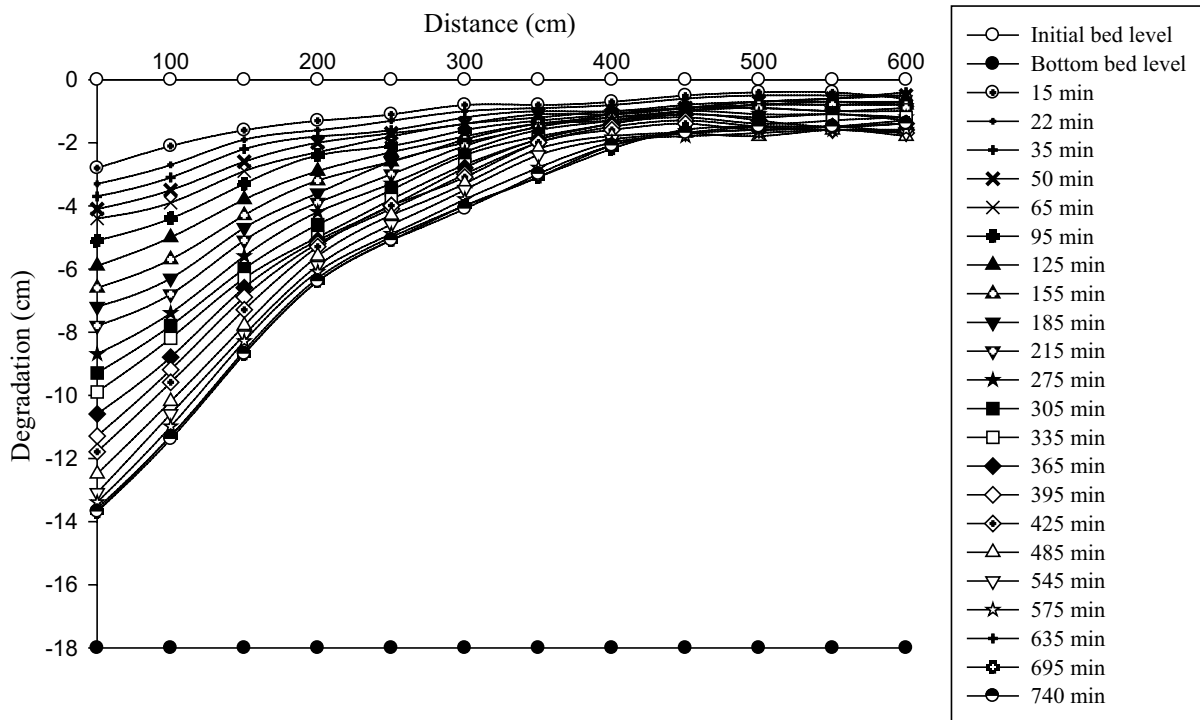
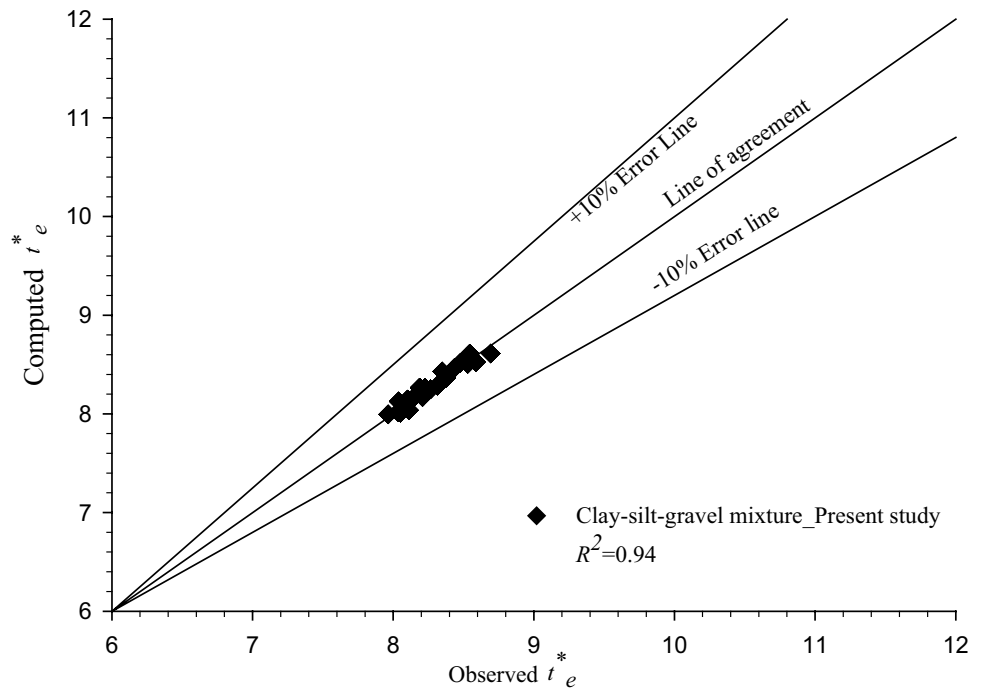


Fig. 18 Bed level variations along the channel bed with time for clay-silt-gravel mixture having 10% clay content at $Q=0.07 \text{ m}^3/\text{s}$, $S_0=0.00721$

After a large number of trials, the following relationship is proposed for the computation of z_{max} for the cohesive sediment mixture.

$$\frac{z_{\text{max}}}{\left(\frac{q^2}{g}\right)^{1/3}} = 1.902(1 + P_c)^{-1.173}(t_e^*)^{0.005} \tag{20}$$

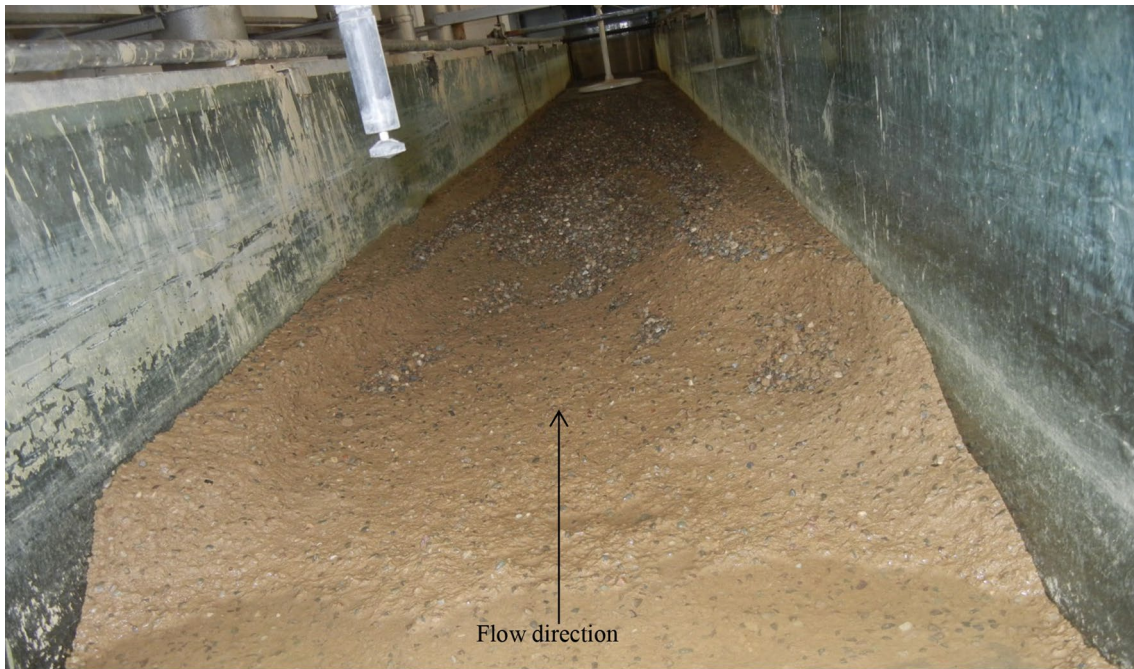
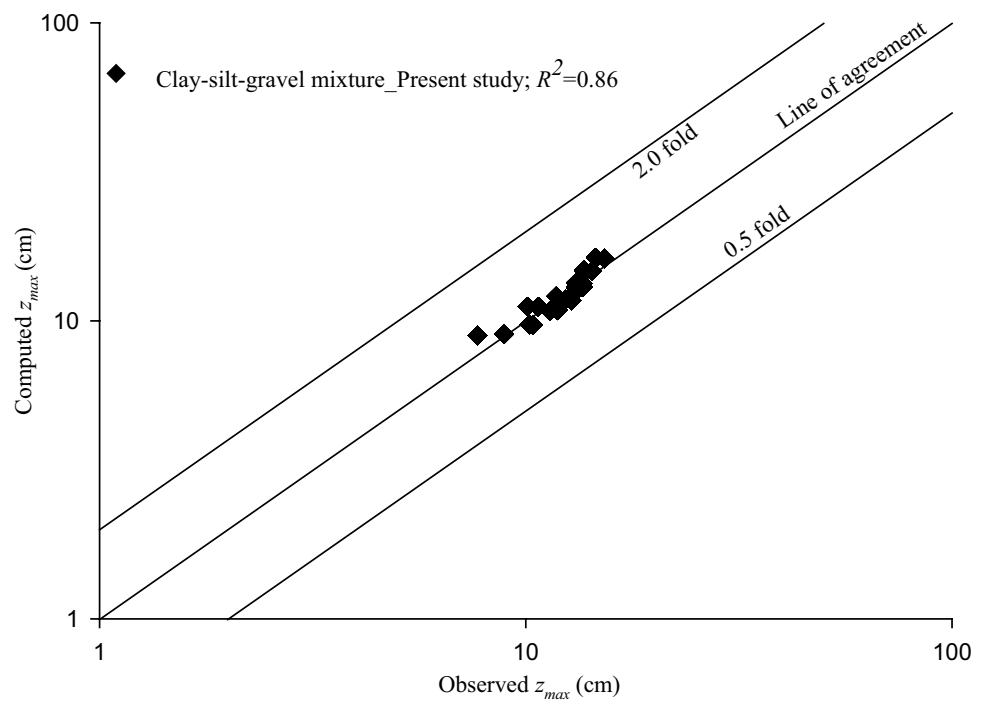


Fig. 19 Bed profile at the end of run for 50% clay content in the mixture at $Q=0.05 \text{ m}^3/\text{s}$, $S_0=0.00946$

Fig. 20 Comparison between computed and observed z_{max}



The computed value of maximum degradation from Eq. (20) for z_{max} shows a good agreement with the observed ones with a good regression coefficient as illustrated in Fig. 20.

After developing the formulation for z_{max} , the relationship for the computation of transient bed profile has been

proposed. Equation (17) can be presented in the dimensionless form as shown below:

$$\frac{z}{z_{\text{max}}} = f\left(\frac{t}{t_e}, \frac{X}{L_{\text{max}}}\right) \tag{21}$$

With the use of the present study data, the following relationship has been proposed for the computation of the bed profile.

$$\frac{z}{z_{\max}} = 1.256 \left(\frac{t}{t_e} \right)^{0.383} e^{-0.235 \frac{x}{L_{\max}}} \tag{22}$$

The proposed formulations show certain limitations like the channel is rectangular in shape, clay varied up to 50%, and the formulation is developed for clay–silt–gravel mixture. A range of parameters like UCS, discharge, and bed slope for hydraulic conditions has been shown in Table 1. Developed formulations for the computation of bed load transport rate and suspended load transport rate and bed degradation profile represented by Eqs. (4, 5, 22), respectively, are applicable with the condition of $0 < \frac{t}{t_e} \leq 1$.

Computed bed profiles with the use of Eq. (22) were compared with the observed data for each percentage of clay (i.e., 10–50%) at different time pints for different flow conditions for the clay–silt–gravel mixture, however, due to space limitation, only few results have been presented as illustrated in Figs. 21, 22, and 23 corresponding to 10%, 30%, and 50% clay content in the mixture of clay–silt–gravel. In Figs. 21, 22 and 23, the initial bed level is indicated by $z = 0$. The comparison between computed and observed bed profiles has been presented, here, for three different time points, i.e., one in initial period of time (after start of run), one towards end time (end of run), one in between initial and end time. A good agreement was found between computed and observed bed profiles for each percentage of clay in clay–silt–gravel mixture as shown in Figs. 21, 22 and 23. Figure 21 corresponds to 10% clay content in the clay–silt–gravel mixture, while Figs. 22 and 23 correspond to 30% and 50% clay content, respectively, in the clay–silt–gravel mixture. Figure 21a, b, c presented bed profiles at $t = 15$ min, $t = 370$ min, and $t = 790$ min, respectively. Similarly, the remaining figures for clay–silt–gravel mixture, i.e., Figs. 22, 23 are present for three different times.

The present study aims to compute the transport rate of bed load and suspended load along with the bed degradation which can be computed using Eqs. (4, 5, 22), respectively. The statistical analysis, for dimensionless bed load transport rate, dimensionless suspended load transport rate, and dimensionless bed degradation, has been carried out using statistical parameters of correlation coefficient (r), root mean square error ($RMSE$), mean absolute percentage of error ($MAPE$), $BIAS$, and scatter index (SI) as per the following equations (Najafzadeh and Lim 2015):

$$r = \frac{\sum_{i=1}^N (Y_{i(\text{Actual})} - \bar{Y}_{(\text{Actual})})(Y_{i(\text{Model})} - \bar{Y}_{(\text{Model})})}{\sqrt{\sum_{i=1}^N (Y_{i(\text{Actual})} - \bar{Y}_{(\text{Actual})})^2 \sum_{i=1}^N (Y_{i(\text{Model})} - \bar{Y}_{(\text{Model})})^2}}$$

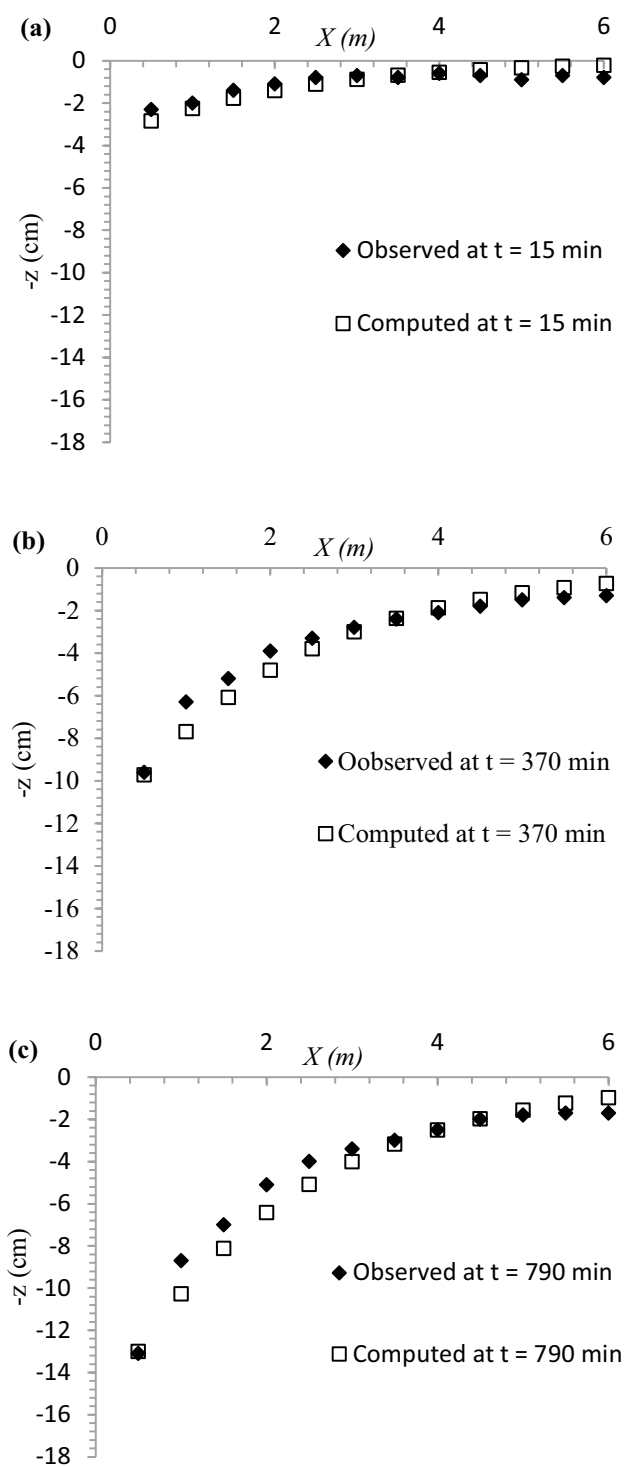


Fig. 21 Comparison between computed and observed bed profile for 10% clay in clay–silt–gravel mixture at $Q=0.05 \text{ m}^3/\text{s}$ and $S_0=0.00721$ at different time "t"

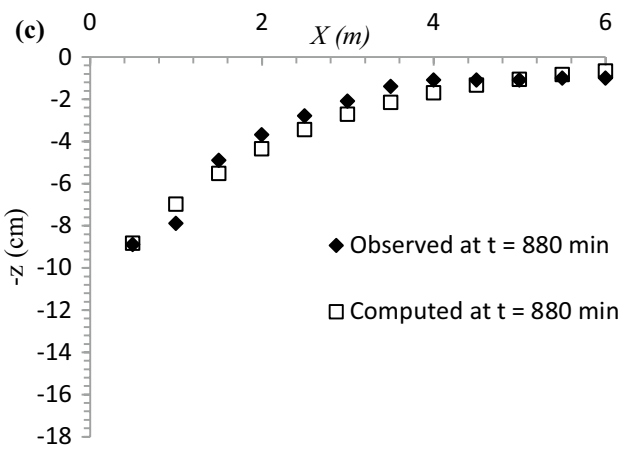
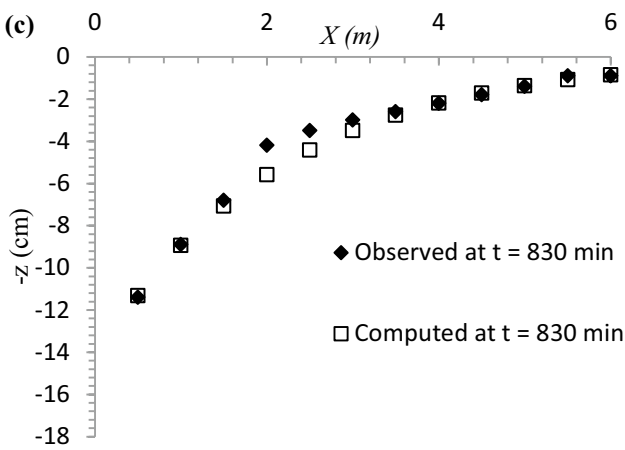
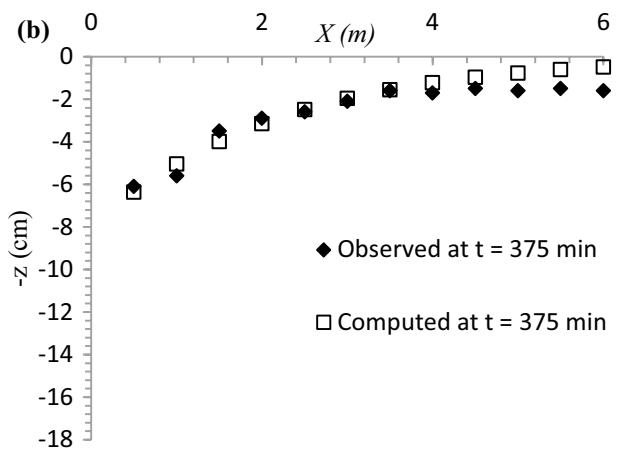
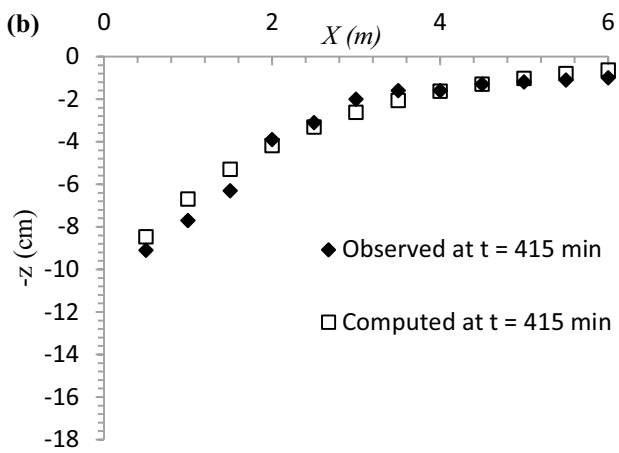
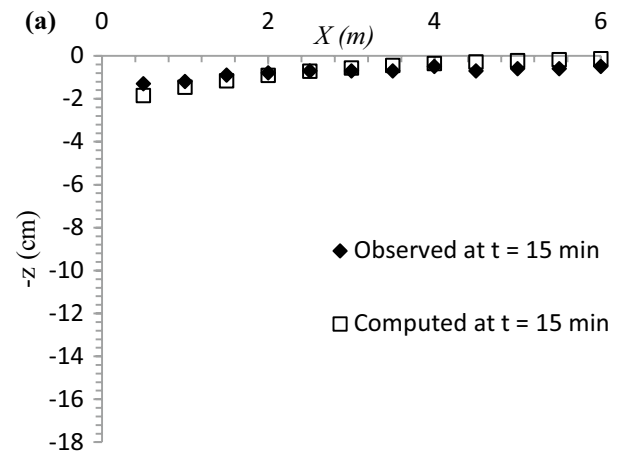
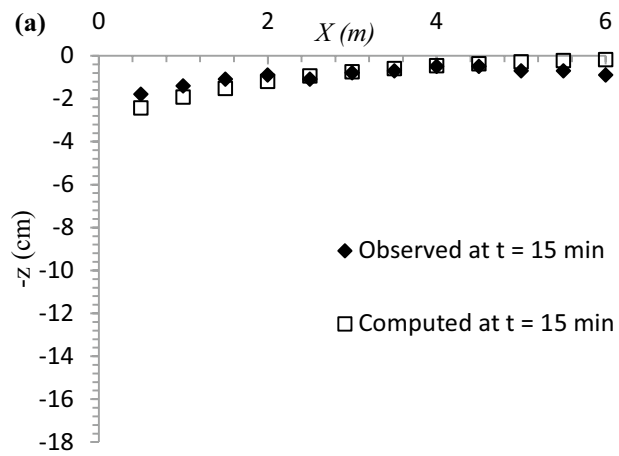


Fig. 22 Comparison between computed and observed bed profile for 30% clay in clay-silt-gravel mixture at $Q=0.05 \text{ m}^3/\text{s}$ and $S_0=0.00721$ at different time "t"

Fig. 23 Comparison between computed and observed bed profile for 50% clay in clay-silt-gravel mixture at $Q=0.05 \text{ m}^3/\text{s}$ and $S_0=0.00946$ at different time "t"

Table 2 Results of statistical parameters

	<i>r</i>	<i>RMSE</i>	<i>MAPE</i>	<i>BIAS</i>	<i>SI</i>
q_{BT}^*	0.98	0.056	0.036	-0.002	0.205
q_{sf}^*	0.98	0.068	0.042	-0.004	0.232
z/z_{max}	0.97	0.058	0.004	0.0007	0.240

$$RMSE = \left[\frac{\sum_{i=1}^N (Y_{i(\text{Model})} - Y_{i(\text{Actual})})^2}{N} \right]^{1/2}$$

$$MAPE = \frac{1}{N} \left[\frac{\sum_{i=1}^N |Y_{i(\text{Model})} - Y_{i(\text{Actual})}|}{\sum_{i=1}^N Y_{i(\text{Actual})}} \times 100 \right]$$

$$BIAS = \frac{\sum_{i=1}^N (Y_{i(\text{Model})} - Y_{i(\text{Actual})})}{N}$$

$$SI = \frac{RMSE}{(1/N) \sum_{i=1}^N Y_{i(\text{Actual})}}$$

The result of statistical analysis is shown in Table 2 which indicates acceptable values for all statistical parameters.

Conclusions

The experimental study was carried out in a laboratory to study the detachment and transport of sediment from a cohesive channel bed made of clay-silt-gravel mixture with clay content that ranged from 10 to 50%. The present study reveals that clay content has a significant effect on the detachment and transport of sediment. The main parameters identified that govern the process of transport rate and transient bed profile were clay content, excess shear stress, and equilibrium time. However, excess shear stress and equilibrium time were influenced by the clay content in the mixture. The experimental study reveals that time taken to reach the stable bed profile varied with clay content and higher clay content in the mixture leads to higher time required for stabilization of bed profile. Equilibrium time was found to increase with the clay content in the mixture. Transport rate of sediment, i.e., bed load as well as suspended load, was found to be higher in the initial period of time, however, it decreases with the passage of time. The initial transport rate of sediment was found to be the function of clay content and excess shear stress. Initial transport rate of sediment was

higher for low clay content, and increases with excess shear stress. Result of experimental study reveals that the maximum degradation occurred at the section of 0.50 m from the start of the mobile bed. Bed degradation was found to be higher in upstream section and decreases towards the downstream section. Degradation of bed was found to be influenced by clay content as well as excess shear stress. Increase in clay content in the mixture leads to lower degradation and increase in excess shear stress resulted in higher degradation. A relationship has been developed for the computation of bed load transport rate of gravel particles, and suspended load transport rate of clay-silt mixture. The relationships were developed as a function of time, equilibrium time, and initial transport rate. Auxiliary relationships were developed for the computation of equilibrium time and initial transport rate of sediment for bed load and suspended load. A relationship has also been developed for the computation of transient bed profile for cohesive mixture of clay-silt-gravel as a function of maximum bed degradation. And the auxiliary relationship was made for the computation of maximum bed degradation. All the developed relationships have a good regression coefficient and were found to be in good agreement with the observed data for the clay-silt-gravel mixture.

Acknowledgements The experimental work presented here is the part of research project funded by the Indian Committee on Surface Water (INCSW), Ministry of Water Resources, Government of India.

References

- Aberle J, Nikora V, Walters R (2004) Effects of bed material properties on cohesive sediment erosion. *Mar Geol* 207:83–93. <https://doi.org/10.1016/j.margeo.2004.03.012>
- Ahmad Z, Singh UK, Kumar A (2018) Incipient motion for gravel particles in clay-silt-gravel cohesive mixtures. *J Soils Sediments* 18:3082–3093. <https://doi.org/10.1007/s11368-017-1869-z>
- ASTM D2487 (2011) Standard practice for classification of soils for engineering purposes (Unified Soil Classification System). ASTM International, West Conshohocken. <https://doi.org/10.1520/d2487-11>
- Brownlie WR (1981) Prediction of flow depth and sediment discharge. In: W. M. Keck Laboratory of Hydraulics and Water Resources, California Institute of Technology, Pasadena, Report no. KH-R-43A
- Debnath K, Nikora V, Elliott A (2007) Stream bank erosion: In situ flume tests. *J Irrig Drain Eng* 133:256–264. [https://doi.org/10.1061/\(ASCE\)0733-9437\(2007\)133:3\(256\)](https://doi.org/10.1061/(ASCE)0733-9437(2007)133:3(256))
- Garde RJ, Ranga Raju KG (2000) Mechanics of sediment transportation and alluvial stream problems, 3rd edn. New Age International, New Delhi
- Houssais M, Lajeunesse E (2012) Bedload transport of a bimodal sediment bed. *J Geophys Res* 117:1–13. <https://doi.org/10.1029/2012JF002490>
- Bureau of Indian Standards (IS) (1975) Determination of dry density of soils in-place by core-cutter method, IS-2720 Part XXIX, New Delhi
- Bureau of Indian Standards (IS) (1991) Determination of unconfined compression strength, IS-2720 Part X, New Delhi

- Jain RK, Kothiyari UC (2009) Cohesion influences on erosion and bed load transport. *Water Resour Res* 45:1–17. <https://doi.org/10.1029/2008WR007044>
- Jain RK, Kothiyari UC (2010) Influence of cohesion on suspended load transport of non-uniform sediments. *J Hydraul Res* 48:33–43. <https://doi.org/10.1080/00221681003696317>
- Jepsen R, Roberts J, Gailani J (2010) Effects of bed load and suspended load on separation of sands and fines in mixed sediment. *J Waterw Port Coast Ocean Eng* 136:319–326. [https://doi.org/10.1061/\(ASCE\)WW.1943-5460.0000054](https://doi.org/10.1061/(ASCE)WW.1943-5460.0000054)
- Khullar NK, Kothiyari UC, Ranga Raju KG (2010) Influence of cohesion on suspended load transport of non-uniform sediments. *J Hydraul Eng* 136:534–543. [https://doi.org/10.1061/\(ASCE\)HY.1943-7900.0000223](https://doi.org/10.1061/(ASCE)HY.1943-7900.0000223)
- Kothiyari UC, Jain RK (2010) Erosion characteristics of cohesive sediment mixtures. In: Dittrich, Koll, Aberle, Geisenhainer (eds) *River Flow 2010*, Bundesanstalt für Wasserbau, pp 815–821. ISBN 978-3-939230-00-7
- Li ZJ, Qian HL, Cao ZX, Liu HH, Pender G, Hu PH (2018) Enhanced bed load sediment transport by unsteady flows in a degrading channel. *Int J Sediment Res* 33:327–339. <https://doi.org/10.1016/j.ijsrc.2018.03.002>
- Misri RL, Garde RJ, Ranga Raju KG (1984) Bed load transport of coarse nonuniform sediment. *J Hydraul Eng* 110:312–328. [https://doi.org/10.1061/\(ASCE\)0733-9429\(1984\)110:3\(312\)](https://doi.org/10.1061/(ASCE)0733-9429(1984)110:3(312))
- Mitchener H, Torfs H (1996) Erosion of mud/sand mixtures. *Coast Eng* 29:1–25. [https://doi.org/10.1016/S0378-3839\(96\)00002-6](https://doi.org/10.1016/S0378-3839(96)00002-6)
- Najafzadeh M, Lim SY (2015) Application of improved neuro-fuzzy GMDH to predict scour depth at sluice gates. *Earth Sci Inform* 8:187–196. <https://doi.org/10.1007/s12145-014-0144-8>
- Owens PN, Batalla RJ, Collins AJ, Gomez B, Hicks DM, Horowitz AJ, Kondolf GM, Marden M, Page MJ, Peacock DH, Petticrew EL, Salomons W, Trustrum NA (2005) Fine-grained sediment in river systems: environmental significance and management issues. *River Res Appl* 21:693–717. <https://doi.org/10.1002/rra.878>
- Paintal AS (1971) A stochastic model of bed load transport. *J Hydraul Res* 9:527–554. <https://doi.org/10.1080/00221687109500371>
- Proffitt GT, Sutherland AJ (1983) Transport of non-uniform sediments. *J Hydraul Res* 21:33–43. <https://doi.org/10.1080/00221688309499448>
- Roberts J, Jepsen R, Gotthard D, Lick W (1998) Effects of particle size and bulk density on erosion of quartz particles. *J Hydraul Eng* 124:1261–1267. [https://doi.org/10.1061/\(ASCE\)0733-9429\(1998\)124:12\(1261\)](https://doi.org/10.1061/(ASCE)0733-9429(1998)124:12(1261))
- Samaga BR, Ranga Raju KG, Garde RJ (1986) Bed load transport of sediment mixtures. *J Hydraul Eng* 112:1003–1018. [https://doi.org/10.1061/\(ASCE\)0733-9429\(1986\)112:11\(1003\)](https://doi.org/10.1061/(ASCE)0733-9429(1986)112:11(1003))
- Shim J, Duan JG (2017) Experimental study of bed-load transport using particle motion tracking. *Int J Sediment Res* 32:73–81. <https://doi.org/10.1016/j.ijsrc.2016.10.002>
- Singh UK, Ahmad Z, Kumar A (2017) Turbulence characteristics of flow over the degraded cohesive bed of clay–silt–sand mixture. *ISH J Hydraul Eng* 23:308–318. <https://doi.org/10.1080/09715010.2017.1313144>
- Swamee PK, Ojha CSP (1991) Bed-load and suspended-load transport of nonuniform sediments. *J Hydraul Eng* 117:774–787. [https://doi.org/10.1061/\(ASCE\)0733-9429\(1991\)117:6\(774\)](https://doi.org/10.1061/(ASCE)0733-9429(1991)117:6(774))
- Waters KA, Curran JC (2015) Linking bed morphology changes of two sediment mixtures to sediment transport predictions in unsteady flows. *Water Resour Res* 51:2724–2741. <https://doi.org/10.1002/2014WR016083>
- Woo H, Julien PY, Richardson EV (1987) Transport of bed sediment in clay suspensions. *J Hydraul Eng* 113:1061–1066. [https://doi.org/10.1061/\(ASCE\)0733-9429\(1987\)113:8\(1061\)](https://doi.org/10.1061/(ASCE)0733-9429(1987)113:8(1061))
- Wu B, Molinas A, Shu A (2003) Fractional transport of sediment mixtures. *Int J Sediment Res* 18:232–247
- Wyss CR, Rickenmann D, Fritschi B, Turowski JM, Weitbrecht V, Boes RM (2016) Measuring bed load transport rates by grain-size fraction using the Swiss plate geophone signal at the Erlenbach. *J Hydraul Eng* 142:1–11. [https://doi.org/10.1061/\(ASCE\)HY.1943-7900.0001090](https://doi.org/10.1061/(ASCE)HY.1943-7900.0001090)

Publisher's Note Springer Nature remains neutral with regard to jurisdictional claims in published maps and institutional affiliations.